Journal of Catalysis **203,** 51–63 (2001)
doi:10.1006/jcat.2001.3311, available online at http://www.idealibrary.com on IDEAL®

Effect of Trichloroethylene on the Photocatalytic Oxidation of Methanol on TiO_2

Darrin S. Muggli,[1] Michael J. Odland, and Lucas R. Schmidt

Department of Chemical Engineering, University of North Dakota, Grand Forks, North Dakota 58202-7107

Received November 28, 2000; revised May 7, 2001; accepted May 11, 2001; published online August 28, 2001

During photocatalytic oxidation (PCO), methanol reacts to formaldehyde, some of which desorbs from TiO_2 at room temperature. Formaldehyde that remains on the surface oxidizes to adsorbed formate, which dehydrogenates to CO_2 in a single step without forming any long-lived intermediates. Adding trichloroethylene (TCE) during PCO of methanol increases the rates of methanol ⇒ formaldehyde and formic acid ⇒ CO_2. Trichloroethylene decreases the rate that formaldehyde oxidizes to formate, however. Adding TCE during PCO of methanol, formaldehyde, and formic acid does not produce any new surface species or reaction pathways. Chlorine radicals that are produced during PCO of TCE may be responsible for the increases in dehydrogenation rates of methanol and formic acid.

Key Words: **methanol; formaldehyde; formic acid; trichloroethylene; photocatalytic oxidation; TiO_2; mixture effects; isotope labeling; transient reaction.**

INTRODUCTION

Volatile organic compounds are regulated by the Clean Air Act of 1990 because they are major contributors to air pollution, both directly through their toxic or malodorous nature and indirectly as ozone precursors (1). Heterogeneous photocatalytic oxidation (PCO) effectively removes a wide range of organic contaminants from waste streams by oxidizing them to environmentally safe compounds (2–15).

Heterogeneous PCO uses a semiconductor catalyst such as TiO_2 and near-UV radiation to oxidize contaminants in both liquid-phase and gas-phase systems at room temperature (2–15). Near-UV irradiation of the semiconductor catalyst excites electrons from the valence to the conduction band, leaving holes behind. These electron–hole pairs migrate to the surface where they initiate redox reactions with organics adsorbed on the surface, completely oxidizing the organics to environmentally safe compounds.

Typically, research on PCO of organics is performed using a single reactant, even though industrial waste streams may contain several organic species (16). The effects of multiple organics in the gas phase can be complex and are not well understood (16–18). Photocatalytic oxidation is an ideal system for studying oxidation of organic mixtures. Transient reaction techniques are easily applied to room temperature PCO because the reaction can be quickly started or stopped by manipulating UV irradiation rather than heating or cooling as in thermal catalysis. In addition, temperature-programmed desorption (TPD) and oxidation (TPO) may be used after transient PCO to identify surface species that do not desorb during PCO (12–14).

Studying mixture effects during PCO is important for a better fundamental understanding of catalyst surface processes, and it is also practical. A potential method to increase PCO efficiency is to add chlorinated organic compounds, such as trichloroethylene (TCE), to the reactor feed. Previous studies have shown that adding TCE and other chlorinated organics as reactants *increased* the PCO rate of certain organics (19–23). However, the PCO rate of some molecules did not change when TCE was added and other molecules reacted more slowly (19). To predict the PCO behavior of TCE/organic mixtures, an increased fundamental understanding of TCE/organic interactions on the catalyst surface is required.

Previous studies added TCE to a reactor feed during PCO of other organics while monitoring reaction rate (19–22). Using a continuous-flow photoreactor, Berman and Dong (22) found that TCE increased the PCO rate of isooctane, methylene chloride, and chloroform. They proposed that TCE produced chlorine radicals, which initiated chain-propagated destruction of these organics.

Lichtin *et al.* (20) studied gas-phase PCO of 14 binary organic mixtures on Degussa P-25 TiO_2. They observed that methanol and CH_2Cl_2 strongly inhibited each other's removal during PCO. Similar results were obtained for TCE/methanol mixtures, but CCl_4 promoted removal of methanol. Methanol inhibited the removal of both CH_2Cl_2 and TCE and they attributed this to PCO intermediates of methanol blocking adsorption sites. They theorized that the reduced reaction rate of TCE in the presence of methanol might explain why TCE does not promote methanol PCO rate.

[1] To whom correspondence should be addressed. Fax: 701-777-3773. E-mail: darrin_muggli@und.nodak.edu.

0021-9517/01 $35.00

d'Hennezel and Ollis (19) used a flow reactor to study the effect of TCE addition on the PCO rate of 18 organics over Degussa P-25 TiO_2. During PCO in the presence of TCE, rate data correlation suggested that chlorine radicals reacted with organics. At low 1-butanol flow rates, adding TCE increased PCO conversion of 1-butanol. When the flow rate of 1-butanol increased from 0.83 to 3 cm^3/s, adding TCE did not change 1-butanol conversion. The authors reasoned that 1-butanol blocked TCE adsorption sites because increasing the flow rate decreased TCE conversion from approximately 86 to 17%. Methanol conversion decreased slightly upon addition of TCE to the feed. The authors suggested that PCO of TCE/alcohols on TiO_2 might proceed similarly to homogeneous photochemical oxidation, in which alcohols undergo chlorine radical attack exclusively at C–H bonds (24). However, they were not able to prove that mechanism for alcohols in their study; high alcohol coverage blocked TCE adsorption sites during steady-state PCO so that TCE conversion was low and few chlorine radicals were generated.

Sauer *et al.* (23) found that perchloroethylene (PCE) and 1,1,3-trichloropropene (TCP) both increased the PCO rate of gas-phase toluene PCO. The apparent quantum yields (molecules reacted per number of incident photons) for both TCP and PCE were greater than one, suggesting the molecules react through chain reaction mechanisms. They concluded that the increase in toluene PCO rate was consistent with a chain reaction mechanism that involved chlorine radical attack as proposed by Luo and Ollis (21) for TCE–toluene mixtures. At low toluene concentrations (up to 22 mg/m^3), TCP enhanced toluene conversion. At high toluene concentrations, however, TCP did not react and conversion of toluene dropped to the same conversion as PCO of toluene alone. During PCO of PCE/toluene mixtures, PCE conversion decreased with reaction time until it reached zero. Toluene conversion also decreased to toluene-only values when PCE conversion was zero. They postulated that PCE oxidizes exclusively through a chain mechanism, which can be completely quenched. However, a stable species may have accumulated on the surface, thereby reducing PCO conversion by blocking adsorption sites.

In this study, methanol and TCE were used to study PCO mixture effects on TiO_2. Trichloroethylene was chosen because its behavior in mixtures is complex in that it can either promote or inhibit PCO of other molecules (19–22). Methanol was used because it is a simple molecule with a high photoefficiency (25), which makes PCO an attractive method for removing methanol from waste streams.

Transient and temperature-programmed reaction techniques were combined with carbon-13 labeling of reactants to study rates and identify surface species during PCO (10–14). Photocatalytic oxidation of TCE/methanol mixtures was performed by adsorbing a monolayer of ^{13}C-methanol ($^{13}CH_3OH$) on the surface, flushing excess $^{13}CH_3OH$ from the gas phase, and injecting TCE quickly after UV-irradiated TiO_2. To determine the effect of TCE addition on each step in the methanol PCO mechanism, transient PCOs were carried out by pulsing TCE into the reactor during PCO of $^{13}CH_3OH$ and each of its PCO intermediates.

Previous studies (19–22) were carried out with TCE and another organic in the gas phase so that competitive adsorption of reactants and site blocking by strongly adsorbed species had to be considered. Indeed, d'Hennezel and Ollis (19) pointed out that the high coverages of alcohols on TiO_2 blocked TCE adsorption sites during steady-state PCO, which made interpretation of their data difficult. Similarly, strongly bound intermediates and products of TCE PCO may block adsorption sites at steady state. An advantage of transient PCO is that competitive adsorption may be controlled by adsorbing different amounts of one organic ($^{13}CH_3OH$, ^{13}C-formaldehyde ($^{13}CH_2O$), or ^{13}C-formic acid ($^{13}CHOOH$)) on fresh TiO_2, flushing excess organic from the gas phase, and pulsing the second organic (TCE or CCl_4) into the gas phase during transient PCO. Furthermore, at steady state a large fraction of the surface may be comprised of PCO intermediates instead of the original reactants (11) and so the effect of TCE for each intermediate, as well as the original reactant, must be considered. Typically during transient PCO, organics (TCE or CCl_4) were pulsed into the reactor quickly after UV irradiation initiated transient PCO of a monolayer of another organic ($^{13}CH_3OH$, $^{13}CH_2O$, or $^{13}CHOOH$) so that the surface was mainly composed of the original adsorbed species and not its PCO intermediates. An added advantage of transient PCO is that each experiment consumes only a small amount (approximately 2 μL) of expensive isotopes ($^{13}CH_3OH$, $^{13}CH_2O$, or $^{13}CHOOH$). This work determines the effect of TCE addition on each step in the methanol PCO mechanism by studying PCO of methanol and each intermediate with and without TCE.

EXPERIMENTAL

The same apparatus was used for PCO, TPD, and TPO. An annular reactor was used to achieve high gas flow rates and uniform UV irradiation of the catalyst. The Pyrex reactor was identical to those used in previous studies (10–14). Approximately 30 mg of Degussa P-25 TiO_2 was coated in a thin layer (average thickness $<0.4\,\mu$m) in the annular region of the reactor. During PCO, 12 UV lamps (Johnlite, F8T5BLB, 8 W) surrounded the reactor to provide uniform UV irradiation of the catalyst. These lamps generate light in the 300 to 500 nm range with a maximum intensity near 360 nm (11). A furnace made of Ni–Cr wire wrapped around a quartz cylinder surrounded the reactor. The end of a 0.5-mm chromel–alumel, shielded thermocouple contacted

the catalyst film during TPD and TPO to provide feedback to the temperature programmer.

Before each isothermal, room-temperature PCO, the reactor was held for 20 min at 723 K in 100 sccm flow of 20% O_2 in He (Praxair, UHP) to create a reproducible surface. After the reactor cooled to room temperature, the organic of interest was injected upstream of the reactor so that it evaporated and adsorbed onto the catalyst. Photocatalytic oxidation was carried out after excess gas phase organic was flushed from the reactor. The UV lights were turned on after a shield was placed between them and the reactor so that the lights would reach a steady-state output before irradiating the surface. During transient PCO of $^{13}CH_3OH$ (Isotec, 99%), $^{13}CH_2O$ (Isotec, 20% aqueous solution), and $^{13}CHOOH$ (Isotec, 99%), a pulse of either TCE (360 μmol/g catalyst, Aldrich, 99.5%) or CCl_4 (330 μmol/g catalyst, Aldrich, 99.9%) was injected into the reactor to simulate PCO of mixtures.

After PCO for a specified time, the UV lights were switched off and either TPD or TPO was carried out. Temperature-programmed oxidation was performed by heating the catalyst in 20% O_2 in He at a constant rate of 1 K/s to 723 K. Temperature-programmed desorption used the same heating rate, but in pure He flow. For both TPD and TPO, the reactor was held at 723 K until no products could be detected in the gas phase.

A Balzers QMS 200 quadrupole mass spectrometer monitored the reactor effluent directly downstream of the reactor. Sampling of the reactor effluent was accomplished using a 25-μm ID fused silica capillary that fed directly to the mass spectrometer ionizer. This sampling system provided high sensitivity and allowed for rapid detection of gas-phase species. The mass spectrometer was interfaced to a computer so that multiple mass peaks could be recorded simultaneously. Calibration was performed by injecting known amounts of each species into the gas flow downstream of the reactor outlet. Integration of the areas under the calibration curves provided a means to convert mass spectrometer signals to reaction rates. The rates of production of gas-phase species were plotted versus time for PCO and temperature for TPD and TPO.

RESULTS

PCO of $^{13}CH_3OH$

Methanol PCO was investigated so that the effect of adding TCE on the methanol PCO mechanism could be determined. Figure 1 shows the formation rates of gas-phase products plotted versus time for transient PCO of a $^{13}CH_3OH$ monolayer without TCE injection. Also shown in Fig. 1 are data for PCO of $^{13}CH_3OH$ with TCE injection, which are described later. In the absence of TCE, adsorbed $^{13}CH_3OH$ oxidized to form gas-phase $^{13}CO_2$ (Fig. 1a) and $^{13}CH_2O$ (Fig. 1b) upon UV irradiation. The $^{13}CO_2$ formation rate reached a maximum of approximately 1.1 μmol/g catalyst/s at 150 s and then decreased. When the UV lights were turned off at 930 s, the $^{13}CO_2$ formation rate quickly dropped to zero, indicating that the formation of $^{13}CO_2$ was reaction limited and not desorption limited. Although the low $^{13}CO_2$ formation rate in Fig. 1a makes the decrease in rate difficult to see, other experiments were performed by turning off the UV lights at early reaction times when the $^{13}CO_2$ formation rate was significantly greater and the $^{13}CO_2$ formation rate dropped quickly after the lights were turned off, in agreement with previous formic acid transient PCO studies (10, 13). Carbon-13-labeled formaldehyde also formed quickly and reached a maximum rate at 130 s, and its formation rate is shown in Fig. 1b with arbitrary units due to difficulties in calibrating the mass spectrometer for formaldehyde (13).

After PCO of a $^{13}CH_3OH$ monolayer for 120 s, TPD was performed to identify intermediates that did not desorb during PCO (Fig. 2). During TPD, a small amount of unreacted methanol desorbed in two peaks at 360 and 590 K. Formaldehyde that had formed and remained on the surface during PCO desorbed at 410 K during TPD. The major TPD product, ^{13}CO that desorbed near 600 K, was attributed to decomposition of either adsorbed formaldehyde or formic acid since both species primarily produce ^{13}CO signals near 600 K during TPD on TiO_2 (13).

Figure 1 shows that formaldehyde is a methanol PCO intermediate since it appeared in the gas phase during methanol PCO and subsequent TPO. Previous studies have shown that formaldehyde oxidizes photocatalytically on TiO_2 to formic acid (2, 3, 13), which subsequently forms CO_2 directly without forming a long-lived intermediate. Therefore, formic acid is also expected to be an intermediate of methanol PCO. Although formic acid adsorbs dissociatively as formate on TiO_2 at room temperature (26–29), we refer to the surface intermediate as formic acid rather than formate to be consistent with other studies (2, 3, 13).

PCO of TCE/$^{13}CH_3OH$

During PCO of a monolayer of $^{13}CH_3OH$, TCE was pulsed into the reactor quickly after UV lights were turned on (Fig. 1a). The carbon-13 products detected in the reactor effluent, $^{13}CO_2$ and $^{13}CH_2O$, were the same as PCO without TCE. After UV irradiation began at 85 s, adsorbed $^{13}CH_3OH$ reacted to form $^{13}CH_2O$ and $^{13}CO_2$ in the gas phase. After TCE was pulsed into the reactor at 97 s (12 s of UV exposure), the rate of $^{13}CO_2$ formation increased more slowly than before the TCE pulse, until it reached a maximum of 0.63 μmol/g catalyst/s. After TCE injection, which lasted approximately 40 s (Fig. 1a), $^{12}CO_2$ formation quickly reached a maximum of 0.24 μmol/g catalyst/s, decreased quickly to 0.1 μmol/g catalyst/s and then decreased more slowly throughout PCO. Although TCE reacted to

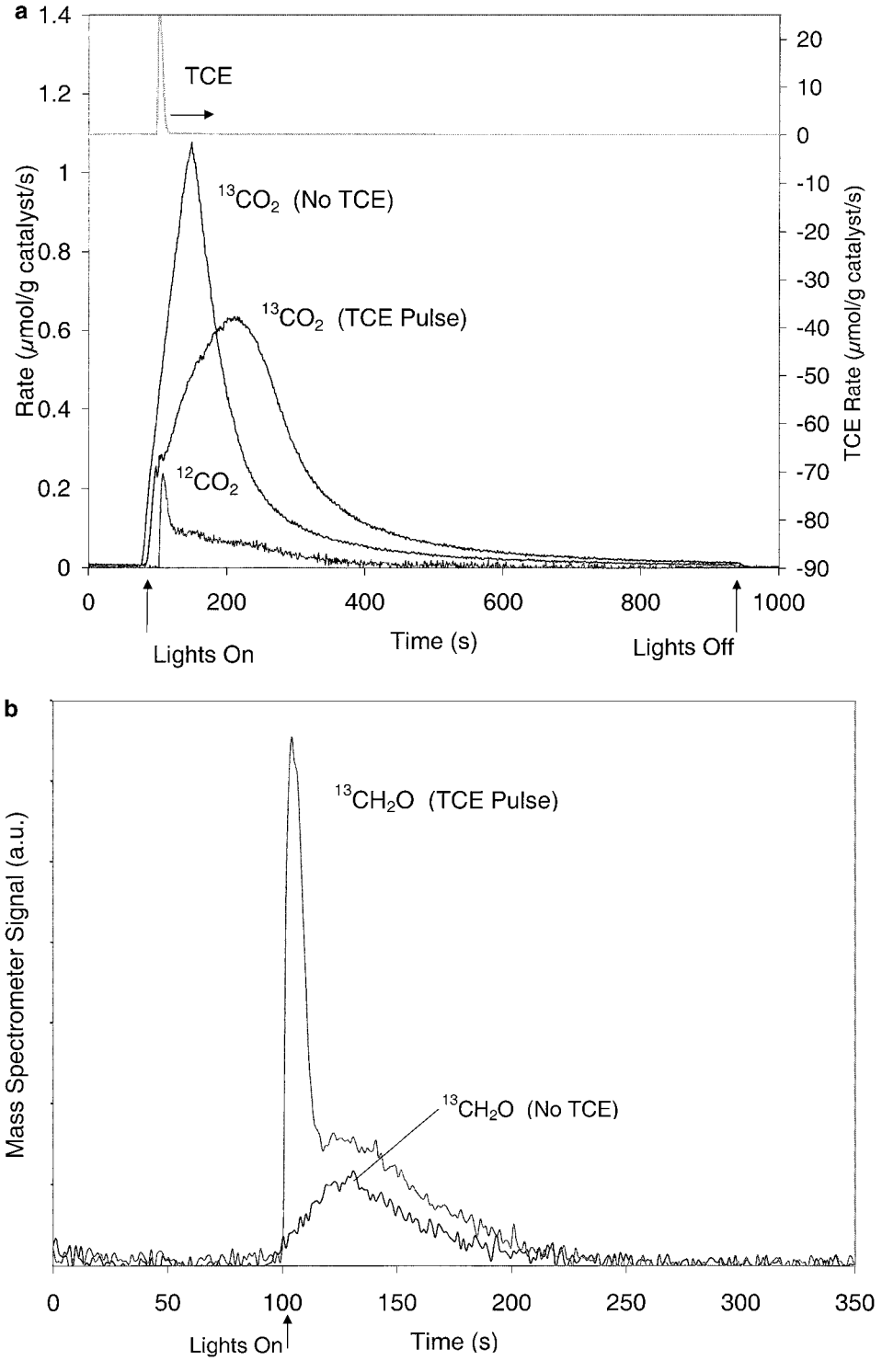

FIG. 1. (a) Formation rates of $^{13}CO_2$ during PCO of $^{13}CH_3OH$ monolayers with and without TCE injection on TiO_2 in 20% O_2. The TCE injection is shown using a secondary *y* axis. (b) Formation rates of $^{13}CH_2O$ in arbitrary units during PCO of $^{13}CH_3OH$ monolayers with and without TCE injection.

form gas-phase dichloracetyl chloride and phosgene, the mass spectrometer was not calibrated for these species.

Figure 1a compares the $^{13}CO_2$ formation rate for the above experiment with that of PCO of a $^{13}CH_3OH$ monolayer without TCE injection. The maximum $^{13}CO_2$ formation rate for PCO of TCE/$^{13}CH_3OH$ was approximately 58% that of PCO of $^{13}CH_3OH$ without TCE injection. In addition, the TCE pulse delayed the maximum $^{13}CO_2$

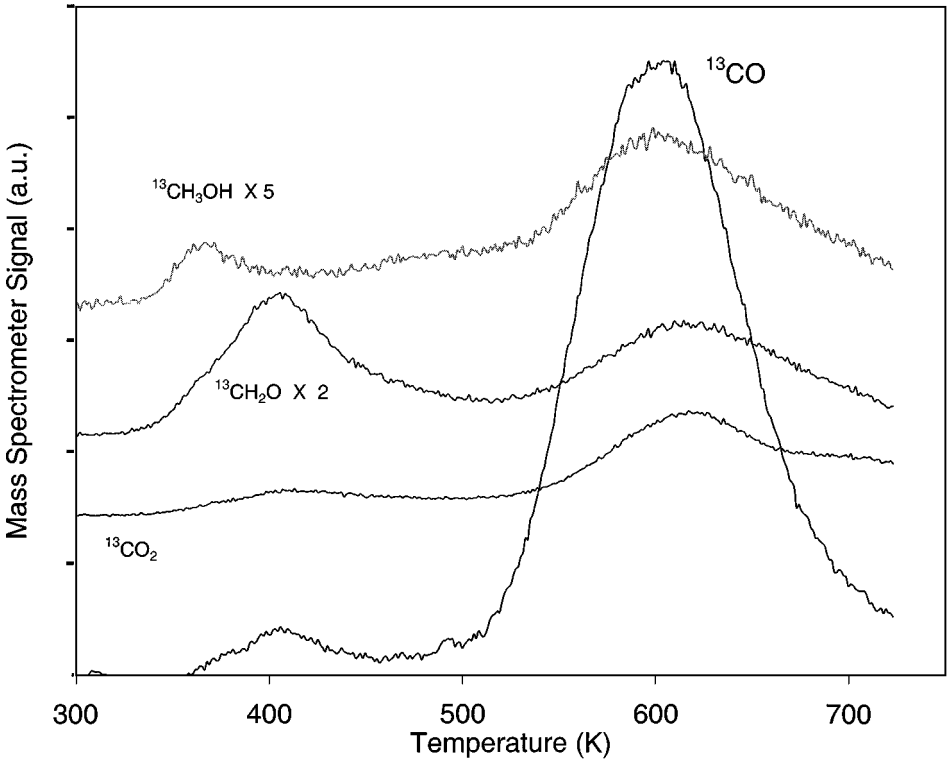

FIG. 2. Temperature-programmed desorption after photocatalytic oxidation of a monolayer of $^{13}CH_3OH$ on TiO_2.

formation rate from 150 to 210 s. Figure 1b shows that TCE increased the maximum $^{13}CH_2O$ formation rate fourfold and the amount of gas-phase $^{13}CH_2O$ produced was twice that of PCO without TCE. Although the mass spectrometer was not calibrated for formaldehyde, CO_2 calibrations for the two experiments shown in Fig. 1 were within 3% of each other, suggesting that the mass spectrometer signals can be used to compare relative formaldehyde rates and amounts.

When TCE was injected after 135 s of transient PCO of a $^{13}CH_3OH$ monolayer, the results were dramatically different than those shown in Fig. 1. The TCE pulse *increased* the $^{13}CO_2$ formation rate from 0.28 to 0.31 μmol/g catalyst/s. Note, however, that the surface compositions for the two experiments were different. When TCE was pulsed into the reactor after 12 s of UV irradation (Fig. 1), only 0.6% of a methanol monolayer reacted to $^{13}CO_2$. After 135 s of PCO, however, 55% of a $^{13}CH_3OH$ monolayer formed $^{13}CO_2$ and a large fraction of the surface species were PCO intermediates ($^{13}CH_2O$ and $^{13}CHOOH$), as was determined by mass balances. Since these results suggest that the PCO intermediates of $^{13}CH_3OH$ react differently than $^{13}CH_3OH$ in the presence of TCE, PCOs with and without TCE were carried out for each intermediate.

PCO of TCE/$^{13}CH_2O$

Since $^{13}CH_2O$ is a PCO intermediate of $^{13}CH_3OH$, the effect of TCE addition during transient PCO of $^{13}CH_2O$ was studied. Pure $^{13}CH_2O$ could not be obtained, and so experiments were carried out using a 20 wt% $^{13}CH_2O$ solution in H_2O. Figure 3 shows the $^{12}CO_2$ and $^{13}CO_2$ formation rates for PCO of adsorbed $^{13}CH_2O$ with TCE injection at 80 s. Injected TCE oxidized to $^{12}CO_2$, reaching a maximum rate of 2.6 μmol/g catalyst/s quickly after TCE was pulsed into the reactor. The $^{13}CO_2$ formation rate quickly reached a maximum of 0.17 μmol/g catalyst/s and decreased slowly until 180 s, after which it decreased more rapidly. Figure 3 also shows the $^{13}CO_2$ formation rate for PCO of a monolayer of adsorbed $^{13}CH_2O$ for comparison. The rate of $^{13}CO_2$ production during PCO without TCE reached a maximum of 0.32 μmol/g catalyst/s at 133 s and then quickly decreased. Injecting TCE during $^{13}CH_2O$ PCO decreased the maximum $^{13}CO_2$ formation rate by 47%. The initial $^{13}CH_2O$ coverages for PCO with and without TCE, calculated by adding the amounts of carbon-containing species detected during PCO and subsequent TPO, were within 5% of each other. No displacement of surface species was observed upon injection of TCE.

PCO of TCE/$^{13}CHOOH$

Previous studies (2, 3, 13) have shown that formaldehyde oxidizes photocatalytically through a formic acid intermediate. Therefore, formic acid is expected to be on the surface during PCO of methanol. Figure 4a shows

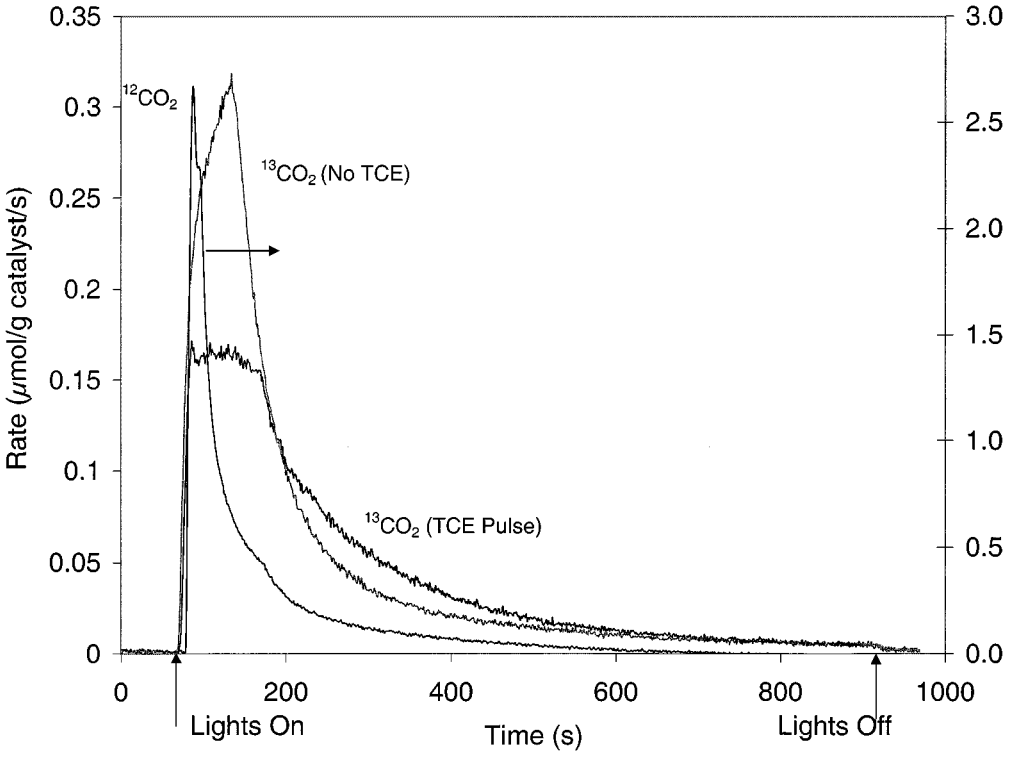

FIG. 3. Photocatalytic oxidation of $^{13}CH_2O$ with and without TCE injection immediately after UV irradiated the surface. Note that the $^{12}CO_2$ formation rate is plotted using the secondary *y* axis.

transient PCO of a monolayer of $^{13}CHOOH$ in which the UV lights were turned on at 70 s and a pulse of TCE was injected at 85 s. Since $^{13}CHOOH$ reacts to $^{13}CO_2$ without forming any long-lived intermediates (2, 3, 13), the $^{13}CO_2$ formation rate reached a maximum (2.1 μmol/g catalyst/s) immediately after UV irradiation. The $^{13}CO_2$ formation rate subsequently decreased to 1.9 μmol/g catalyst/s and then *increased* to 2.5 μmol/g catalyst/s when TCE was pulsed into the reactor. After TCE was pulsed into the reactor, the maximum $^{13}CO_2$ formation rate was 19% greater than the initial $^{13}CO_2$ formation rate even though the coverage of formic acid was approximately 10% lower when TCE was injected. Photocatalytic oxidation of TCE to $^{12}CO_2$ quickly reached a maximum rate of 1.7 μmol/g catalyst/s after TCE was injected and then decreased throughout PCO.

Figure 4b shows the early stages of $^{13}CO_2$ formation from Fig. 4a, as well as PCO of a $^{13}CHOOH$ monolayer without TCE for reference. The initial maximum $^{13}CO_2$ production rates for both experiments differed by less than 5%, indicating the experiments were reproducible.

Temperature-Programmed Oxidations

After 120 s PCOs were carried out for $^{13}CH_3OH$, $^{13}CH_2O$, and $^{13}CHOOH$, TPOs were performed to characterize the species that did not react or desorb during PCO (Figs. 5–7). Also shown in Figs. 5–7 are TPO spectra after 120 s PCOs of $^{13}CH_3OH$, $^{13}CH_2O$, and $^{13}CHOOH$, each with an immediate injection of TCE during PCO. Comparing the TPO spectra with and without TCE injection during PCO allows any new surface species resulting from the TCE pulse to be identified. One complication of comparing the aforementioned TPO spectra, however, is that they might be different because of interactions between adsorbed species during TPO. Furthermore, PCO of TCE has been reported to chlorinate TiO_2 (21, 23, 30–33), so that the catalyst surface would be different after PCO with and without TCE injection. To account for these effects, TPO was performed for a surface in which the organic of interest ($^{13}CH_2O$ or $^{13}CHOOH$) was adsorbed after a 600-s PCO of a TCE pulse.

TPO after methanol PCOs. Figure 5 shows ^{13}CO, $^{13}CH_2O$, and $^{13}CH_3OH$ desorption during TPO after $^{13}CH_3OH$ PCO with and without TCE injection. When TPO was performed by adsorbing $^{13}CH_3OH$ after TCE PCO, no ^{13}CO, or $^{13}CH_2O$ desorbed. Therefore, the TPO spectra for this experiment are not plotted in Fig. 5. Carbon dioxide desorbed in a small broad peak near 600 K, but since $^{13}CO_2$ desorption was similar for all TPO experiments, it is not shown in Figs. 5–7 for clarity. Temperature-programmed oxidation after PCO of TCE/$^{13}CH_3OH$ showed that ^{13}CO desorbed at lower temperatures than during TPO after

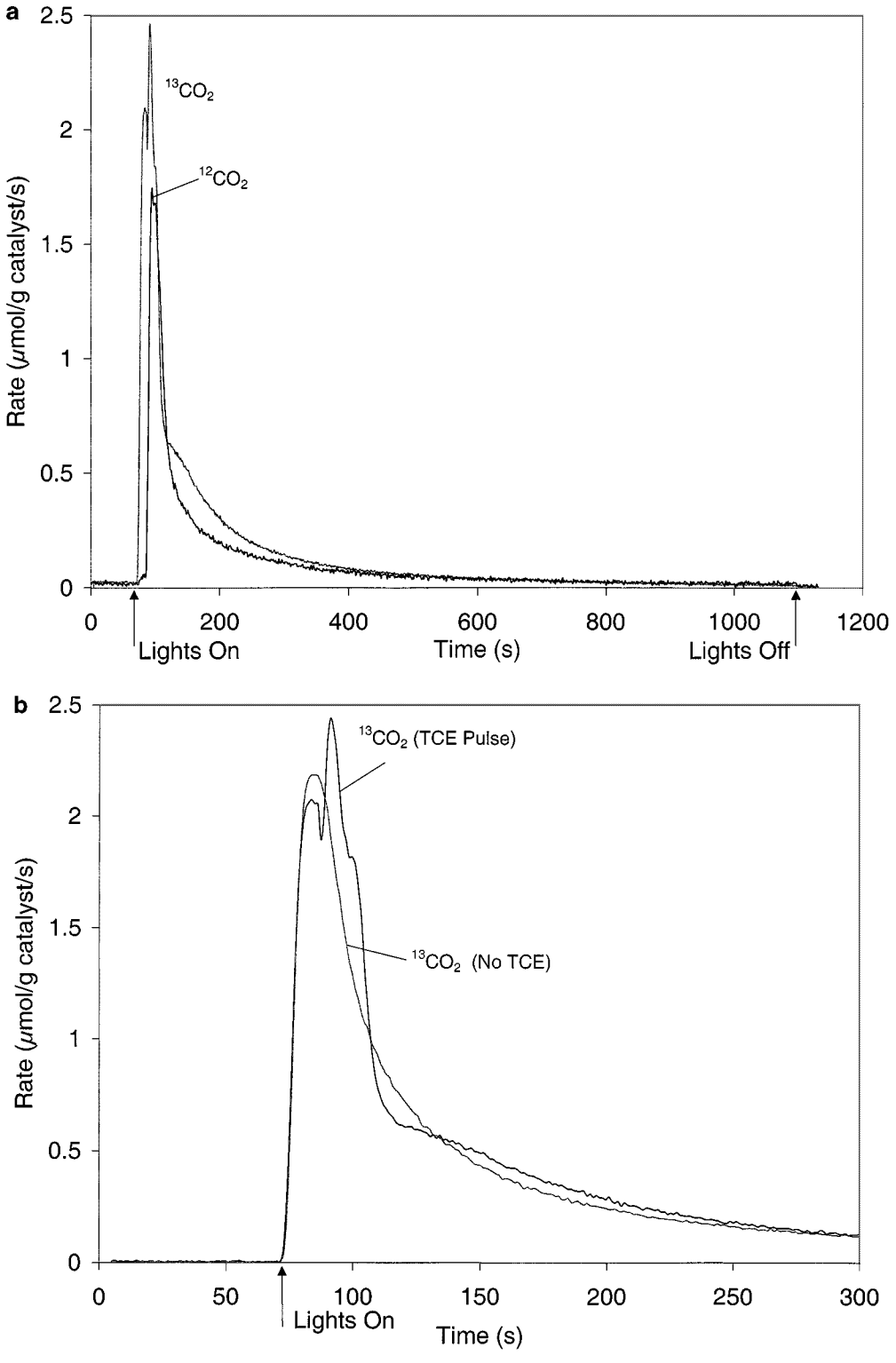

FIG. 4. (a) Formation rates of $^{13}CO_2$ and $^{12}CO_2$ during photocatalytic oxidation of a $^{13}CHOOH$ monolayer with TCE injection. (b) Early stages of PCO of $^{13}CHOOH$ with TCE injection. Also shown in (b) is PCO of a $^{13}CHOOH$ monolayer without TCE for reference.

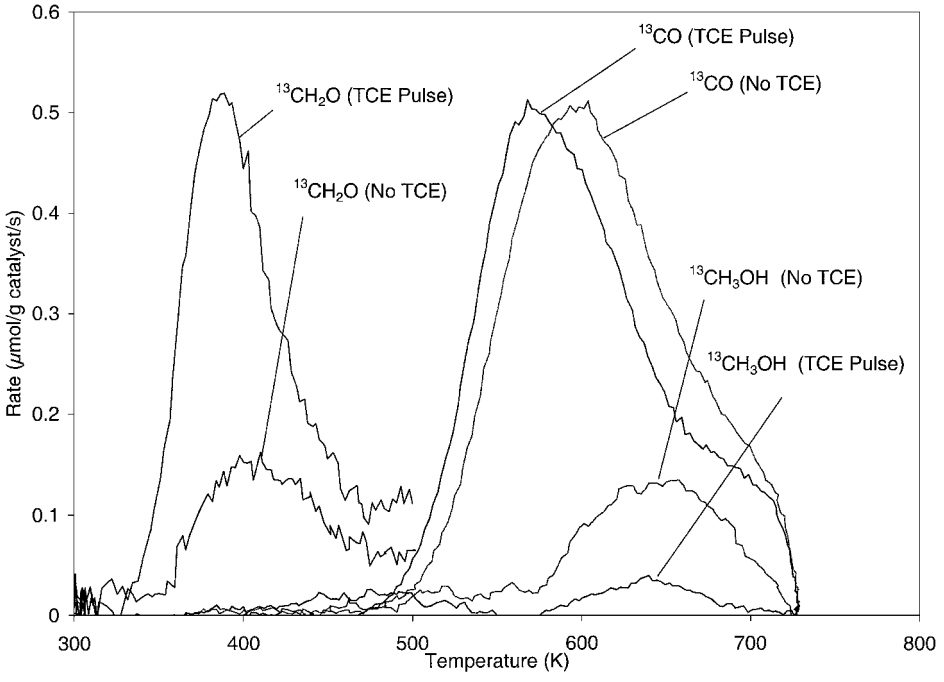

FIG. 5. Desorption spectra for TPO that followed PCO of $^{13}CH_3OH$ monolayers with and without TCE injection during PCO. The desorption rates of $^{13}CH_2O$ and $^{13}CH_3OH$ are in arbitrary units.

PCO of $^{13}CH_3OH$ without TCE. The maximum ^{13}CO desorption rates were 570 and 600 K for TPO after PCO with and without TCE, respectively.

Figure 5 shows $^{13}CH_3OH$ and $^{13}CH_2O$ desorption rates in arbitrary units for PCO with and without TCE. The amount of unreacted $^{13}CH_3OH$ that desorbed during TPO after PCO of TCE/$^{13}CH_3OH$ was approximately one-half of that after PCO of $^{13}CH_3OH$. Adding TCE during $^{13}CH_3OH$ PCO increased the amount of $^{13}CH_2O$ that desorbed during subsequent TPO by a factor of 1.6. Both the low-temperature formaldehyde desorption (Fig. 5) and the appearance of ^{13}CO near 600 K were attributed to adsorbed formaldehyde. However, the ^{13}CO desorption near 600 K may also be due in part to adsorbed formic acid.

TPO after formaldehyde PCOs. Figure 6 shows TPO spectra after $^{13}CH_2O$ PCO with and without TCE injection. Also shown is TPO that was performed by adsorbing $^{13}CH_2O$ after PCO of a pulse of TCE. Similar to methanol, injecting TCE during $^{13}CH_2O$ PCO caused ^{13}CO to desorb at lower temperatures during subsequent TPO (Fig. 6a). The maximum ^{13}CO desorption rates were 545 and 580 K after PCO of $^{13}CH_2O$ with and without TCE, respectively. Also, the amount of formaldehyde that desorbed near 400 K after PCO of TCE/$^{13}CH_2O$ was 1.5 times that after PCO without TCE (Fig. 6b). The spectra for TPO performed by adsorbing $^{13}CH_2O$ after pulse PCO of TCE were similar to TPO after TCE/$^{13}CH_2O$ PCO; ^{13}CO desorbed with a maximum rate at 555 K and similar amounts of $^{13}CH_2O$ desorbed near 400 K.

TPO after formic acid PCOs. Figure 7 shows ^{13}CO desorptions for TPO after PCO of $^{13}CHOOH$ and TCE/$^{13}CHOOH$, as well as TPO performed by adsorbing $^{13}CHOOH$ after pulse PCO of TCE. Similar to the results presented for $^{13}CH_2O$, ^{13}CO desorbed at lower temperature during TPO after PCO of TCE/$^{13}CHOOH$ than for TPO after PCO of $^{13}CHOOH$. Temperature-programmed oxidation that was performed by adsorbing $^{13}CHOOH$ after pulse PCO of TCE resulted in a ^{13}CO desorption that was similar to that for TPO after PCO of TCE/$^{13}CHOOH$. Both of these experiments produced ^{13}CO maximum desorption rates 30 K lower than TPO after PCO of a monolayer of $^{13}CHOOH$.

PCO of CCl_4/Methanol

Experiments were carried out by injecting pulses of CCl_4 into the reactor during PCO of $^{13}CH_3OH$, $^{13}CH_2O$, and $^{13}CHOOH$. For all experiments, CCl_4 did not react to form gas-phase products during PCO. Moreover, no carbon-12 species were detected during subsequent TPO, indicating that no strongly bound intermediates formed and remained adsorbed during PCO. Furthermore, no change in the rate of any of the carbon-13-labeled reactants was observed, as was expected since CCl_4 did not react during PCO. These results contrast those of Lichtin *et al.* (20),

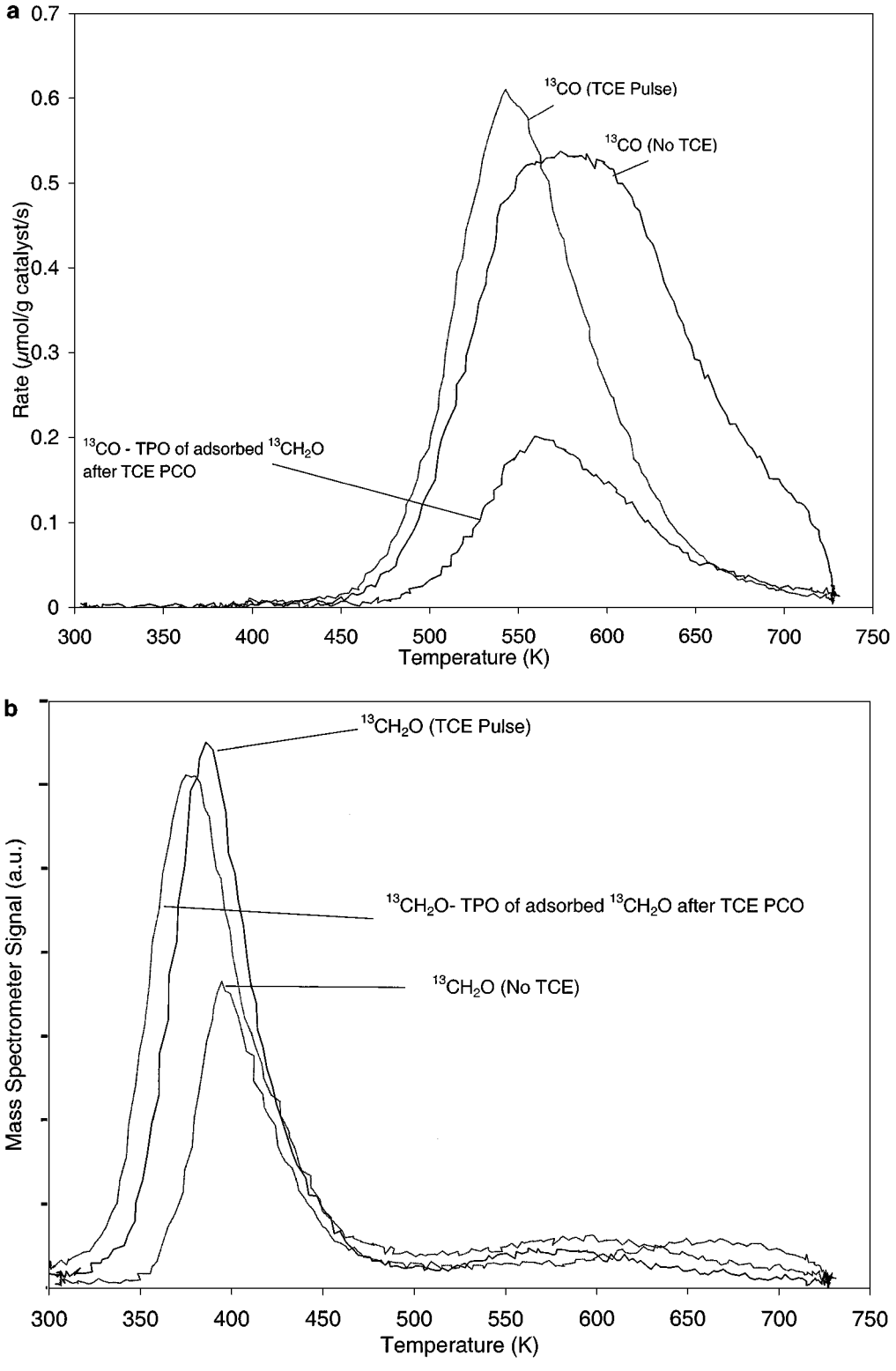

FIG. 6. (a) Desorption of ^{13}CO and (b) $^{13}CH_2O$ during TPO that followed PCO of $^{13}CH_2O$ with and without TCE injection during PCO. Also shown is TPO that was performed by adsorbing $^{13}CH_2O$ after PCO of a pulse of TCE.

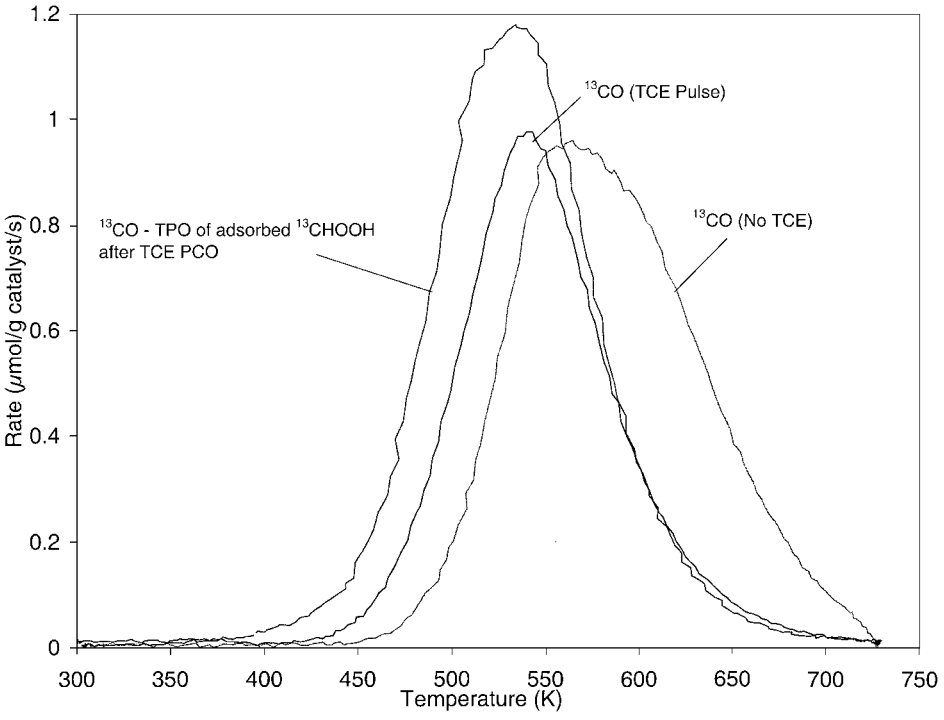

FIG. 7. Desorption of ^{13}CO during TPO that followed PCO of monolayers of $^{13}CHOOH$ with and without TCE injection during PCO. Also shown is ^{13}CO desorption during TPO that was performed by adsorbing $^{13}CHOOH$ after PCO of a pulse of TCE.

who observed that CCl_4 promoted the removal of methanol during PCO.

DISCUSSION

Methanol PCO Mechanism

The first step in the proposed mechanism (Reaction [1]) is oxidation of methanol to formaldehyde. As shown in Fig. 1, adsorbed $^{13}CH_3OH$ oxidized photocatalytically to form gas-phase $^{13}CH_2O$, which desorbed at early reaction times. In addition, TPD after PCO showed that $^{13}CH_2O$ was on the surface during PCO. Figure 2 shows $^{13}CH_2O$ desorption near 400 K and ^{13}CO formation near 600 K, both of which indicate that $^{13}CH_2O$ was on the surface during PCO.

Previous studies have shown that formaldehyde oxidizes photocatalytically through a formic acid intermediate (2, 3, 13). In particular, Nimlos *et al.* (3) detected formic acid in the gas phase using FTIR during PCO of formaldehyde. Figure 2 shows ^{13}CO desorption near 600 K, which may be in part due to adsorbed formic acid (13, 26, 27, 29). Therefore, formaldehyde is expected to produce adsorbed formic acid during PCO.

Muggli *et al.* (13) showed that formic acid oxidizes to CO_2 in a single step during PCO without forming any long-lived intermediates, in agreement with others (2, 3). Therefore, the proposed reaction pathway shows that methanol produces formaldehyde, which oxidizes to CO_2 through a formic acid intermediate: (note that O_2 consumption and H_2O production are not shown in the mechanism below for clarity.)

$$CH_3OH \Rightarrow CH_2O \Rightarrow HCOOH(\text{formate}) \Rightarrow CO_2. \quad [1]$$

This mechanism agrees with one proposed by Liu *et al.* (34) for PCO of methanol on MoO_3/TiO_2 at elevated temperature. They proposed that methanol adsorbs dissociatively to form surface methoxide on both MoO_3 and TiO_2. On TiO_2, they proposed that adsorbed methoxide forms formaldehyde, which subsequently produces adsorbed formate. They proposed that condensation of surface formate produced significant amounts of gas-phase methyl formate during steady-state PCO experiments carried out above 403 K and with 4% methanol in the gas phase. For the transient room-temperature PCOs of the current study, no methyl formate formed, in agreement with other room-temperature PCO studies (2, 10–14) in which formate was on the surface.

TCE Mixture Effects

Previous studies proposed that PCO of TCE and other chlorinated organics produces chlorine, which abstracts hydrogen from other organics (19–23). Sauer *et al.* (23) proposed that photo-induced holes (h^+), hydroxyl radicals ($OH^\bullet$), or oxygen atoms react with chlorinated organics to form chlorine radicals that subsequently oxidize adsorbed

organics. To explain the increase in toluene PCO rate upon addition of TCE, Luo and Ollis (21) proposed that chlorine radicals abstract hydrogen atoms from the methyl group of toluene via the reaction

$$Cl^{\bullet} + \phi CH_3 \Rightarrow \phi CH_2^{\bullet} + HCl. \quad [2]$$

Based on previous work (35) in which atomic chlorine was found to react significantly slower with benzene than with toluene, the authors concluded that chlorine atoms abstract hydrogen faster from alkyl groups than from aromatic rings. Similarly during PCO, d'Hennezel and Ollis (19) found that TCE addition did not enhance the benzene PCO rate but increased PCO rates of toluene, *m*-xylene, and ethylbenzene. Therefore, they also concluded that chlorine radicals, produced during TCE PCO, preferentially abstracted hydrogen from alkyl groups rather than aromatic ring hydrogen. The results presented here are consistent with PCO of TCE producing chlorine radicals that abstract hydrogen from other organics. The effect of TCE addition on each step in the methanol PCO mechanism is discussed herein.

Methanol ⇒ formaldehyde. Figure 1b shows that TCE addition during $^{13}CH_3OH$ PCO increased the formation rate of gas-phase $^{13}CH_2O$. The increased $^{13}CH_2O$ formation rate is not due to displacement by TCE. When TCE was pulsed over monolayers of adsorbed $^{13}CH_3OH$, $^{13}CH_2O$, and $^{13}CHOOH$ in the dark, no displacement of adsorbed organics was observed. In addition, Fig. 5 shows that injecting TCE during $^{13}CH_3OH$ PCO increased the amount of weakly adsorbed $^{13}CH_2O$ by approximately 80%. Since PCO with TCE produced more adsorbed $^{13}CH_2O$, the increased rate of production of gas-phase $^{13}CH_2O$ is not due to $^{13}CH_2O$ displacement. A portion of the increase in the amount of $^{13}CH_2O$ that desorbed near 400 K during TPO after PCO with TCE may be due to PCO products of TCE blocking sites so that less weakly bound formaldehyde readsorbs during TPO. However, Fig. 5 shows less unreacted methanol was on the surface after PCO of TCE/methanol than PCO of methanol without TCE, which indicates that TCE increased the rate that methanol forms formaldehyde.

Formaldehyde ⇒ formic acid. Figure 3 shows that TCE decreases the $^{13}CO_2$ formation rate during PCO of $^{13}CH_2O$. Since adding TCE increases the rate of $^{13}CHOOH$ oxidation to $^{13}CO_2$ (Fig. 4), but it decreases the rate that $^{13}CH_2O$ produces $^{13}CO_2$ (Fig. 3), TCE addition must decrease the rate that $^{13}CH_2O$ forms $^{13}CHOOH$.

A direct comparison of the formaldehyde PCO rate to those of methanol and formic acid was not possible, since an aqueous $^{13}CH_2O$ solution was used so that a monolayer of $^{13}CH_2O$ could not be produced. Adsorbed H_2O is expected to diminish the effect of TCE since experiments carried out by injecting TCE over a surface of coadsorbed H_2O and $^{13}CH_3OH$ showed that TCE still decreased the PCO rate, but not as dramatically as when $^{13}CH_3OH$ was adsorbed without H_2O. Since the rate of $^{12}CO_2$ formation was also lower when water was coadsorbed with $^{13}CH_3OH$, apparently H_2O blocked TCE adsorption sites. Therefore, TCE should decrease the $^{13}CO_2$ formation rate more for a monolayer of $^{13}CH_2O$ without adsorbed water.

Note that in contrast to the other steps in the methanol PCO mechanism, oxidation of $^{13}CH_2O$ to form $^{13}CHOOH$ is not a simple dehydrogenation. Therefore, dehydrogenation of adsorbed formaldehyde by chlorine radicals may present a different reaction pathway than PCO without TCE. This may explain the decreased rate of CO_2 production during formaldehyde PCO, if this reaction pathway produces a stable species that reacts slowly during PCO. However, no new species were detected in the gas phase during formaldehyde PCO or subsequent TPO. The carbon-13 products that desorbed during TPO after PCO of TCE/formaldehyde were the same as those for formaldehyde alone. This indicates that TCE most likely did not produce a new reaction pathway for $^{13}CH_2O$ PCO. The decrease in formaldehyde PCO rate upon addition of TCE is more likely the result of TCE PCO chlorinating the TiO_2 surface, which is discussed later.

Formic Acid ⇒ CO_2. The last step in the proposed methanol PCO mechanism is dehydrogenation of adsorbed formic acid to CO_2. After PCO of $^{13}CHOOH$ with and without TCE, subsequent TPO showed no intermediates on the surface. This indicates that formic acid dehydrogenates directly to CO_2 during PCO with and without TCE.

The increased rate of formic acid PCO upon TCE addition (Fig. 4) is consistent with chlorine radicals dehydrogenating formic acid to form CO_2. The shape of the $^{13}CO_2$ formation curve during PCO of TCE/$^{13}CHOOH$ (Fig. 4) suggests two processes are occurring. Before TCE was injected, the $^{13}CO_2$ formation rate had already reached a maximum and started to decrease. Pulsing TCE caused a sharp increase in the $^{13}CO_2$ formation rate. Subsequently, the $^{13}CO_2$ formation rate dropped sharply as the rate that TCE oxidized to $^{12}CO_2$ quickly decreased. Between 100 and 130 s, $^{13}CO_2$ and $^{12}CO_2$ formation rates decreased by 73 and 75%, respectively. Since both $^{13}CO_2$ and $^{12}CO_2$ rates dropped at nearly the same rate during this 30-s interval, the decrease in rate is attributed to fewer chlorine radicals produced by PCO of TCE. After 130 s, the $^{13}CO_2$ formation rate decreased more slowly than that of $^{12}CO_2$. Presumably, chlorine radicals from TCE PCO were being produced more slowly after 130 s so that PCO without chlorine radicals contributed significantly to the total $^{13}CO_2$ production rate.

The maximum $^{13}CO_2$ rate for PCO with a TCE pulse was greater than that of a monolayer of formic acid (Fig. 4). This indicates that the increase in rate cannot be explained by displacement of formic acid to more active sites during

the TCE pulse. Moreover, no displacement of adsorbed formic acid was observed when TCE was pulsed into the reactor. Also, TCE did not displace adsorbed $^{13}CO_2$ since CO_2 does not significantly adsorb on Degussa P-25 at room temperature (13).

When TCE was pulsed into the reactor at 260 s, significantly more TCE reacted to form $^{12}CO_2$ and since formic acid coverage was lower after 260 s, the $^{13}CO_2$ formation rate increased less than when TCE was pulsed earlier. Therefore, the increase in $^{13}CO_2$ rate upon TCE injection is not due to a product of TCE oxidation that cracked in the mass spectrometer to interfere with the $^{13}CO_2$ signal. Although a small signal at a mass-to-charge ratio 45 was detected during PCO of a pulse of TCE, it was not large enough to significantly change any of the $^{13}CO_2$ rates presented here.

Adsorbed Species during PCO

The only differences in TPO spectra after PCO with and without TCE were increases in the amounts of weakly bound formaldehyde during PCO of methanol and formaldehyde (Figs. 5 and 6b) and shifts in ^{13}CO desorptions to lower temperatures for all molecules (Figs. 5–7). A stable surface species that produced ^{13}CO at lower temperatures during TPO may have formed during PCO with TCE, but this shift to lower temperatures was also observed for ^{13}CO desorption after TCE/formic acid PCO. A stable reaction intermediate is not expected to form during PCO of TCE/formic acid since adding TCE increased the formic acid PCO rate. Therefore, the shift in ^{13}CO desorption temperature after PCO of TCE/$^{13}CH_3OH$, TCE/$^{13}CH_2O$, and TCE/$^{13}CHOOH$ is most likely not due to the formation of a new stable intermediate caused by the TCE pulse. Also, the decrease in ^{13}CO desorption temperature cannot be explained by intermediates of TCE PCO blocking readsorption sites during TPO; ^{13}CO does not appreciably adsorb on TiO_2 (30, 36) so that readsorption of ^{13}CO during TPO is unlikely.

The shift in ^{13}CO desorption temperature may be due to reactions between the PCO intermediates of methanol and those of TCE during TPO, since TPO performed by adsorbing $^{13}CH_2O$ and $^{13}CHOOH$ after TCE PCO produced similar shifts to lower temperature in ^{13}CO desorption. Alternatively, TiO_2 may become chlorinated during PCO of TCE thereby changing the surface and the subsequent TPO spectra.

Surface Chlorination of TiO_2

Several studies (19–23, 32) proposed that surface chlorination leads to the formation of active species that react with adsorbed organics during PCO. Sauer *et al.* (23) postulated that the TiO_2 surface could be partially or completely converted to an active Ti–O_x–Cl_y surface during PCO of chlorinated organics, in agreement with other studies (21, 30–33). The authors postulated that exposing a chlorinated surface to UV irradiation could evolve a singlet oxygen ($^1O_2$), as reported by Munuera *et al.* (33), and this species could then react with adsorbed organics during PCO as proposed by Braun *et al.* (37). Luo and Ollis (21) also suggested that TiO_2 may become sufficiently chlorinated during PCO of TCE to produce a new surface. They suggested that the chlorinated surface could increase PCO rate by forming chlorine radicals or reducing the electron–hole recombination rate.

d'Hennezel *et al.* (32) found that prechlorinating TiO_2 with HCl gave similar results as adding TCE during PCO of aromatics. They concluded that, although prechlorination of the surface produced chlorine radicals that affected the PCO rate of certain molecules and changed the relative amounts of intermediates, it did not produce any new species. Similarly in the current study, no new reaction pathways were identified for PCO of $^{13}CH_3OH$, $^{13}CH_2O$, and $^{13}CHOOH$ in the presence of TCE, in agreement with d'Hennezel *et al.* (32).

Chlorination of TiO_2 after PCO of TCE was observed by Larson and Falconer (36), who used X-ray photoelectron spectroscopy to detect two forms of surface chlorine on catalysts used for gas-phase PCO of TCE. For our experiments in which TCE was oxidized photocatalytically with and without other organics present, HCl desorbed in two peaks centered at 380 and 600 K during TPD after PCO of TCE and other organics. Desorption of HCl continued up to the maximum TPD temperature of 723 K and dropped to zero as the reactor was held at this temperature for approximately 20 min.

Reactive species ($Cl^{\bullet}$, $^1O_2$, etc.) produced by a chlorinated surface could explain the increase in the PCO rates of methanol $\Rightarrow$ formaldehyde and formic acid $\Rightarrow$ CO_2. Furthermore, surface chlorination of TiO_2 might explain why the rate that formaldehyde oxidizes to formic acid decreases when TCE is added during PCO. Primet *et al.* (31) showed that chlorine in CCl_4 replaces lattice oxygen of TiO_2 at 400 K. They proposed a model of the chlorinated surface in which chlorine replaced half of the surface oxygen atoms. A similar chlorination of TiO_2 during PCO of TCE could also replace lattice oxygen with chlorine. If formaldehyde oxidizes to formic acid through a Mars Van Krevlen mechanism in which lattice oxygen is abstracted and subsequently replenished from the gas phase, then decreasing the amount of lattice oxygen by chlorination of TiO_2 would most likely reduce the formaldehyde PCO rate. Indeed, Liu *et al.* (34) proposed that a neighboring O^{2-} surface anion initiates nucleophilic attack on the C atom in CH_2O to produce surface formate during PCO. Similarly, Busca *et al.* (38) proposed that adsorbed formaldehyde undergoes attack from nucleophilic lattice oxygen at room temperature on TiO_2 without UV light.

CONCLUSIONS

Methanol oxidizes photocatalytically on TiO_2 to CO_2 through formaldehyde and formic acid intermediates. During photocatalytic oxidation, trichloroethylene increased the rates of methanol ⇒ formaldehyde and formic acid ⇒ CO_2 but decreased the formaldehyde ⇒ formic acid rate. Adding TCE during PCO of methanol, formaldehyde, and formic acid did not produce any new surface species or reaction pathways for methanol PCO. The results presented here are consistent with an active species produced by TCE PCO, perhaps chlorine radicals, increasing the rate that methanol and formic acid dehydrogenate to formaldehyde and CO_2, respectively.

Temperature-programmed oxidations showed that PCO of TCE produces strongly bound chlorine species. Chlorination of the TiO_2 surface appears to slow the rate that formaldehyde oxidizes during PCO, perhaps by decreasing the availability of lattice oxygen. Carbon tetrachloride did not react when it was injected over monolayers of methanol, formaldehyde, and formic acid because these species blocked CCl_4 adsorption sites; therefore, CCl_4 did not change the PCO rate of these organics. Trichloroethylene adsorbed weakly to TiO_2 and therefore it did not displace adsorbed methanol, formaldehyde, or formic acid from the surface. Adsorbed water blocked TCE adsorption sites and therefore decreased the TCE PCO rate.

ACKNOWLEDGMENTS

Acknowledgment is made to the Donors of the Petroleum Research Fund, administered by the American Chemical Society, for support of this research.

REFERENCES

1. Papaefthimiou, P., Ioannides, T., and Verykios, X. E., *Appl. Catal. B Environ.* **3–4**, 175 (1997).
2. Sauer, M. L., and Ollis, D. F., *J. Catal.* **149**, 81 (1994).
3. Nimlos, M. R., Wolfrum, E. J., Brewer, M. L., Fennell, J. A., and Bintner, G., *Environ. Sci. Technol.* **30**, 3102 (1996).
4. Vorontsov, A. V., Barannik, G. B., Snegurenko, O. I., Savinov, E. N., and Parmon, V. N., *Kinet. Catal.* **38**, 84 (1997).
5. Peral, J., and Ollis, D. F., *J. Catal.* **136**, 554 (1992).
6. Blake, N. R., and Griffin, G. L., *J. Phys. Chem.* **92**, 5697 (1988).
7. Cunningham, J., Hodnett, B. K., and Walker, A., *Proc. R. Irish Acad.* **77**, 411 (1977).
8. Kennedy, J. C., III, and Datye, A. K., *J. Catal.* **179**, 375 (1998).
9. Falconer, J. L., and Magrini-Bair, K. A., *J. Catal.* **179**, 171 (1998).
10. Muggli, D. S., and Falconer, J. L., *J. Catal.* **191**, 318 (2000).
11. Muggli, D. S., and Falconer, J. L., *J. Catal.* **180**, 111 (1998).
12. Muggli, D. S., and Falconer, J. L., *J. Catal.* **175**, 213 (1998).
13. Muggli, D. S., McCue, J. T., and Falconer, J. L., *J. Catal.* **173**, 470 (1998).
14. Muggli, D. S., Larson, S. A., and Falconer, J. L., *J. Phys. Chem.* **100**, 15886 (1996).
15. Jacoby, W., Nimlos, M., and Blake, D., *Environ. Sci. Technol.* **29**, 1223 (1995).
16. Dangi, S., and Abraham, M., *Ind. Eng. Chem. Res.* **36**, 1979 (1997).
17. Gangwal, S. K., Mullins, M. E., Spivey, J. J., and Carffrey, P. R., *Appl. Catal.* **36**, 231 (1988).
18. Barresi, A. A., and Baldi, G., *Chem. Eng. Comm.* **123**, 17 (1993).
19. d'Hennezel, O., and Ollis, D. F., *J. Catal.* **167**, 197 (1996).
20. Lichtin, N. N., Avudaithal, M., Berman, E., and Grayfer, A., *Solar Energy* **56**, 377 (1996).
21. Luo, Y., and Ollis, D. F., *J. Catal.* **163**, 1 (1996).
22. Berman, E., and Dong, J., *in* "The Third International Symposium Chemical Oxidation: Technology for the Nineties" (W. W. Eckenfelder, A. R. Bowers, and J. A. Roth, Eds.), p. 183. Technomic Publishers, Chicago, 1993.
23. Sauer, M. L., Hale, M. A., and Ollis, D. F., *J. Photochem. Photobiol.* **88**, 169 (1995).
24. Phillips, L. A., and Raupp, G. B., *J. Mol. Catal.* **77**, 297 (1992).
25. Miller, R., and Fox., R., *in* "Photocatalytic Purification and Treatment of Water and Air" (D. F. Ollis and H. Al-Ekabi, Eds.), p. 573. Elsevier, New York, 1993.
26. Henderson, M. A., *J. Phys. Chem.* **99**, 15253 (1995).
27. Henderson, M. A., *J. Phys. Chem. B* **101**, 221 (1997).
28. Onishi, H., Aruga, T., and Iwasawa, Y., *J. Catal.* **146**, 557 (1994).
29. Kim, K. S., and Barteau, M. A., *Langmuir* **6**, 1485 (1990).
30. Kim, K. S., Barteau, M. A., and Farneth, W. F., *Langmuir* **4**, 533 (1988).
31. Primet, M., Basset, J., Matheiu, M. V., and Prettre, M., *J. Phys. Chem.* **74**, 2868 (1970).
32. d'Hennezel, O., Pichat, P., and Ollis, D. F., *J. Photochem. Photobiol.* **118**, 197 (1998).
33. Munuera, B., Navio, A., and Rives-Arnau, V., *J. Chem. Soc., Faraday Trans.* **77**, 2747 (1981).
34. Liu, Y. C., Griffin, G. L., Chan, S. S., and Wachs, I. E., *J. Catal.* **94**, 108 (1985).
35. Wallington, T. J., Skewes, L. M., and Siegl, W. O., *J. Photochem. Photobiol. A: Chem.* **45**, 588 (1998).
36. Larson, S. A., and Falconer, J. L., *Appl. Catal. B.* **4**, 325 (1994).
37. Braun, A. M., Maurette, M.-T., and Oliveros, E., "Photochemical Technology," Wiley, New York 1991.
38. Busca, G., Lamotte, J., Lavalley, J. C., and Lorenzelli, V., *J. Am. Chem. Soc.* **109**, 5197 (1987).